Off-Lattice Monte Carlo Simulations of Polymer Melts Confined between Two Plates. 2. Effects of Chain Length and Plate Separation

Sanat K. Kumar*

Department of Material Science and Engineering, Polymer Science Program, The Pennsylvania State University, University Park, Pennsylvania 16802

Michele Vacatello[1] and Do Y. Yoon

IBM Research Division, Almaden Research Center, 650 Harry Road, San Jose, California 95120. *Received June 23, 1989; Revised Manuscript Received October 13, 1989*

ABSTRACT: In an earlier paper,[2] we presented a Monte Carlo simulation technique in the canonical ensemble to model the static properties of polymer melts confined between two impenetrable plates. In this paper we consider the effects of variations in polymer chain length and plate separation on the detailed, microscopic conformations of polymer chains in the film. Three plate separations, corresponding roughly to R_G (the unperturbed radius of gyration of chains), $2R_G$, and $10R_G$, were examined for chains with 100 connected beads (i.e., n_b = 100). Also, polymers of three different n_b's, 50, 100, and 200, were studied at the same plate separation, 51 segment diameters, to examine the effects of changes in polymer chain length. We find that the influence of a surface on chain conformations in a polymer melt are restricted to only those segments that are confined to within approximately twice the segment diameter from the surface, independent of chain length and plate separation. All other segments assume random conformations and orientations. This feature, as well as the detailed comparison of the "train sequences" at the surfaces, is in surprisingly good agreement with the predictions of the mean-field lattice theory. The bead-density profile, as obtained from the simulations, exhibits enhanced packing near the surfaces that is apparently independent of plate separation and chain length. The only effect of decreasing plate separation is manifested in more symmetric chain shapes due to an increased presence of bridging conformations. On the other hand, the preference of chain ends to be located at the surface is enhanced with increasing chain length but remains unaffected by plate separation. Implications of these results on the surface forces in a melt and the variation of surface tension of a polymer melt with molecular weight are also discussed.

1. Introduction

The behavior of polymeric systems confined into thin films is a situation that has numerous practical consequences. The use of polymers as lubricant films and as thin dielectric layers in microelectronic devices and the stabilization of colloidal suspensions with adsorbed polymer chains represent typical examples of this problem. Previously,[2] we presented the results of an off-lattice Monte Carlo simulation of a polymer melt with the segment density corresponding to a polyethylene melt at a temperature of 400 K. We considered a monodisperse polymer with 100 (n_b) connected beads confined into a film of thickness, D = 51 segment diameters ($\approx 10R_G$, where R_G is the unperturbed radius of gyrations of the chains.) In this paper we extend these calculations by performing two more sets of simulations for systems consisting of chains of n_b = 100: these are for plate separations corresponding roughly to R_G and $2R_G$ of the unperturbed chains. We examine the effects of changes in plate separation on the properties of single chains and beads as functions of their positions relative to the surface. In addition, we also consider the properties of two other confined, monodisperse melts at the same plate separation (51 segment diameters): one comprising of chains of length n_b = 50, while the other has chains of length 200 beads, and the effects of variations in chain length on the microscopic chain properties in the film are examined subsequently.

2. Model

The model simulated and the Monte Carlo technique employed have been described in detail in ref 2. Hence we provide only a brief description here. The basic system that was considered in these simulations was a box of dimensions N_x, N_y, and N_z units in the x, y, and z directions, respectively. Periodic boundary conditions were assumed in the x and y directions as illustrated in Figure 1. The faces of the box in the z direction were considered to be impenetrable and hence corresponded to neutral walls. A polymer molecule was assumed to be a necklace of n_b connected beads. The bond length was set to be equal to the diameter of a bead, σ, which in this case corresponds to 4.6 Å (see below). It was assumed that there was no energetic interaction between covalently connected beads, while all other neighbors interacted with a truncated 6–12 Lennard-Jones potential

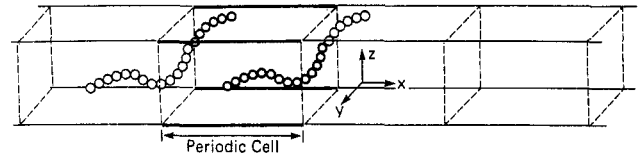

Figure 1. A schematic representation of the system that was simulated by the Monte Carlo scheme.

$$E(r_{ij}) = -\epsilon\left[\frac{2\sigma^6}{r_{ij}^6} - \frac{\sigma^{12}}{r_{ij}^{12}}\right] \quad (r_{ij} < r_0)$$
$$= 0 \quad (r_{ij} \geq r_0) \qquad (1)$$

Here, r_{ij} denotes the separation between beads i and j, σ and ϵ are the distance and energy parameters associated with the potential model, respectively, and r_0 is the distance at which the potential is truncated. As in the earlier work[2] σ was assigned a value of 4.6 Å, ϵ = 100 cal/

0024-9297/90/2223-2189$02.50/0

Table I
Systems Simulated in This Work

chain length[a]	plate separation[b]	box size (x, y dimens)[b]	overall density[c]
100	51	50 × 50	0.98
100	11	50 × 50	0.91
100	6	50 × 50	0.83
50	51	50 × 50	0.98
200	51	50 × 50	0.98

[a] Chain length is in units of number of beads, n_b. [b] All distances are in units of σ. [c] Bead density is expressed in units of beads/σ^3.

Table II
Chain Statistics in the Central Region as a Function of Polymer Chain Length[a-c]

chain length	$\langle R^2\rangle^{1/2}$	$\langle R_G^2\rangle^{1/2}$	C_n	$\langle R^2\rangle/\langle R_G^2\rangle$
50	8.64 (0.19)	3.52 (0.06)	1.49 (0.07)	6.01 (0.45)
100	12.40 (0.41)	5.09 (0.12)	1.54 (0.12)	5.94 (0.67)
200	18.14 (1.69)	7.54 (0.41)	1.60 (0.30)	5.79 (1.07)

[a] $\langle R^2\rangle^{1/2}$ and $\langle R_G^2\rangle^{1/2}$ are in units of σ. [b] All data obtained from the center of film of thickness 51σ. [c] Numbers in brackets are the standard deviations associated with each quantity. These standard deviations arise since each of these quantities assume a range of values that may be characterized as a distribution.

mol and the potential truncation distance, r_0, was set equal to σ. The chains were assumed to be freely jointed otherwise; i.e., no additional potentials were utilized to describe the preference of the chains to exist in specific conformations. The total density corresponding to this system was roughly 1 bead/σ^3 which is comparable to the density in molten polyethylene at 400 K (assuming that each bead corresponds to roughly 3.5 methylene units). The simulations were conducted at 400 K. In Table I we list the dimensions of the simulated systems and the appropriate density conditions that were employed in this work. The systems in consideration were studied under conditions of constant temperature, volume, and total number of particles. The simulations were then conducted in the Canonical ensemble through the use of a Metropolis importance sampling technique.[2]

In the first set of simulations three different plate separations (D) were considered for chains of $n_b = 100$. These were 6σ, 11σ, and 51σ. (For comparison, the unperturbed R_G of the chains is ca. 5.1σ.[2]) Subsequently, we studied a system consisting of chains of $n_b = 50$ at a plate separation of 51σ, and also a system comprised of chains of $n_b = 200$ at the same plate separation. In all cases, 10 different equilibrium structures were obtained and all results reported represent averages over these 10 structures.

3. Results and Discussion

3.1. Chains in the Central Region. For the thickest film, corresponding to a plate separation of 51σ, there exists a region in the middle of the film where the polymer chains assume their unperturbed conformations.[2] We have computed the root-mean-square (RMS) end-to-distance, $\langle R^2\rangle^{1/2}$, the RMS radius of gyration, $\langle R_G^2\rangle^{1/2}$, and characteristic ratios, C_n, for these unperturbed chains at the three different chain lengths examined. These results are reported in Table II. It may be noted that the characteristic ratios, C_n, are essentially independent of chain length and, within the standard deviations inherent with the calculation of this quantity, agree with the value of 1.38 computed analytically for the unperturbed chains.[2] Additionally, it may be seen that the ratio, $\langle R^2\rangle/\langle R_G^2\rangle$ is nearly equal to the expected value of 6 in all cases.[6] This verifies that the chains in the center of the film, in all cases, are unperturbed and bulklike. An important conclusion of these results is to establish the equilibrium nature of the structures generated.

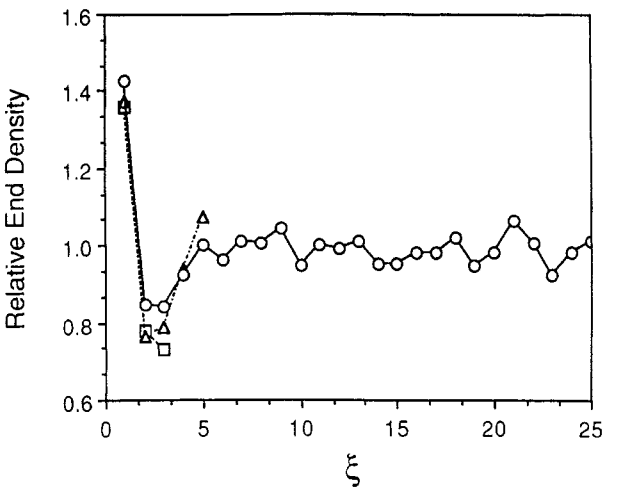

Figure 2. Relative density of chain ends as a function of absolute, normalized distance, ξ, from the plates. Chain end density has been normalized by the value expected in an unperturbed bulk. All data are for chains of $n_b = 100$ with (○) for $D = 51\sigma$, (△) for D = 11σ, and (□) for $D = 6\sigma$.

3.2. Polymers of $n_b = 100$ at Different Plate Separations. We begin by examining the results obtained on the polymer melt film comprising of chains of 100 connected beads at three different film thicknesses: 6σ, 11σ, and 51σ. All properties were examined as a function of their absolute, normalized z distance from the wall, $\xi = |z - z_w|/\sigma$, where z_w is the z position of the surface. Note is made of the fact that the results that are to be reported in this section are obtained by averaging data over bins of thickness 1σ in the z direction. In contrast, our earlier work[2] and also results to be presented for polymers of different chain lengths (see section 3.3) are data obtained by averaging over bins of size 2σ. This smaller bin size has been employed in this case to obtain detailed information for chain properties even in the smallest plate separations (i.e., for $D = 6\sigma$).

In Figure 2 we examine the density of chains ends (normalized by the value expected in an isotropic phase), $\rho_e(\xi)$, as a function of their absolute, normalized distance from the wall, ξ. This quantity, $\rho_e(\xi)$, will assume a value of unity in an isotropic phase. In all the three cases examined, the density of chain ends at the surface is higher than the isotropic value. Also, within the accuracy of the simulation results, this enhancement at the surface is essentially independent of the plate separation.

As has been explored in earlier work,[2] the density of chain ends reaches its isotropic value when one proceeds a distance ca. $2R_G$ from the surface. This can be verified by examination of the results corresponding to $D = 51\sigma$ in Figure 2. In the other two plate separations, however, the density of ends never reaches its isotropic value since the films are only R_G and $2R_G$ thick, respectively. Further examination of Figure 2 shows that as one decreases the film thickness, it appears as if the regions in the middle are squeezed out leaving behind only the outer sections of the profile. Surprisingly, almost no synergistic effects are noted. Some of these features were also observed previously in the lattice simulations of ten Brinke et al.[4] However, their simulations, which were conducted at a polymer filling of only 80%, showed much smaller enhancements of the end density at the surface.[4] For example, in corresponding units, ten Brinke et al.[4]

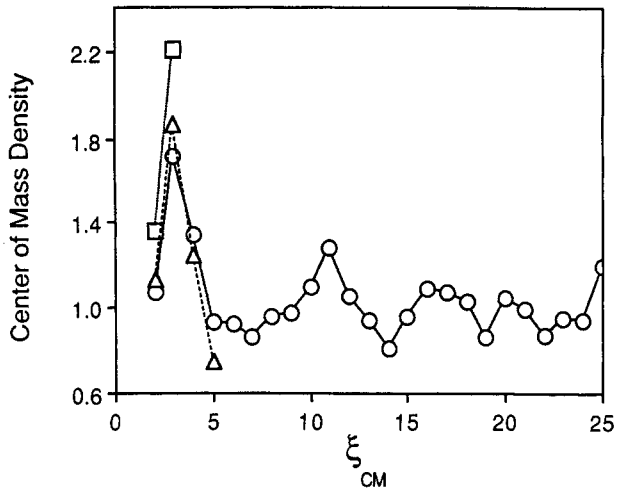

Figure 3. Relative density of centers of mass as a function of their absolute, normalized distance, ξ_{CM}, from the plates. Center of mass density has been normalized by the value expected in an unperturbed bulk. All data are for chains of $n_b = 100$ with (○) for $D = 51\sigma$, (△) for $D = 11\sigma$, and (□) for $D = 6\sigma$.

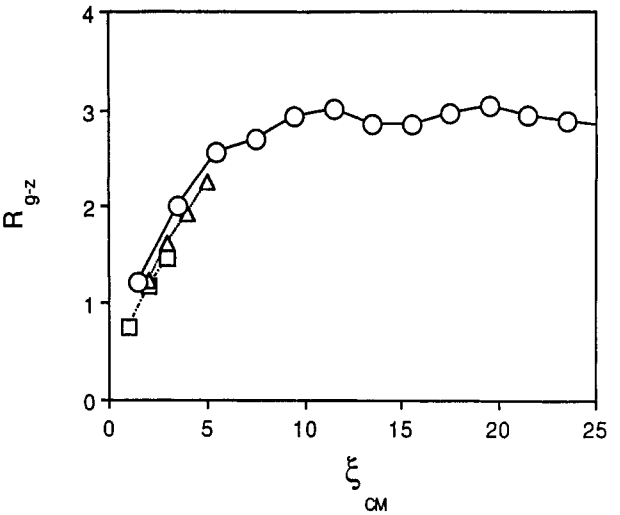

Figure 4. z component of the radius of gyration of chains as a function of the absolute, normalized center of mass distance, ξ_{CM}, from the plates. All data are for chains of $n_b = 100$ with (○) for $D = 51\sigma$, (△) for $D = 11\sigma$, and (□) for $D = 6\sigma$.

report that the end density at the surface is 1.08, independent of chain length and plate separation. In comparison, Figure 2 shows that the end density at the surface, as obtained from an off-lattice simulation, is ca. 1.4 times larger than in an isotropic melt. Since there are no density restrictions that are built into an off-lattice simulation, they allow one to obtain estimates for the properties of an interfacial system that are more reliable than information that can be obtained from a lattice calculation. In the rest of this paper, at several junctures, we will attempt to examine the applicability and shortcomings of lattice calculations in this context and also compare these results to the predictions of the more realistic off-lattice simulations.

3.2.1. Chain Properties as Functions of Their Center of Mass Position. Having examined the density of ends near the surface we proceed to analyze the distribution of centers of mass of the chains in the film along the z direction. The center of mass in the z direction is the z component of the average vector position of all the beads in a chain.[2] In Figure 3 we plot the density distribution of centers of mass, $\rho_{CM}(\xi_{CM})$, as a function of their absolute, normalized distance from the plates, ξ_{CM} (= $|z_{CM} - z_w|/\sigma$), for the three different plate separations that have been examined. As usual, the densities have been normalized by the value expected in an isotropic, bulk phase. As reported in the earlier work,[2] the center of mass density in the thickest film (i.e., 51σ) is depleted in the immediate vicinity of the surface and reaches its peak value at a distance of roughly 3σ from the walls. This quantity approaches its isotropic value when one proceeds roughly $2R_G$ from the surface, which corresponds to the distance at which the melt does not feel the presence of the surface any longer. The results obtained in the case of the two other plate separations (6σ and 11σ) conform to these general trends. As observed in the density of chain ends one eliminates the bulk regions of the density profiles in the films as the two plates are squeezed together. It should be noted that the maximum value of $\rho_{CM}(\xi_{CM})$ increases slightly as one reduces the film thickness. Almost no additional effects are noted, suggesting that, at least at these distances, the presence of one plate does not modify significantly the interface at the other wall. This is an unexpected result since the interface for single-chain properties has earlier been shown to be roughly $2R_G$ in thickness,[2] and the plate separations in two of the simulated systems are comparable to, or smaller than, this dimension. These results, again, are qualitatively in good agreement with the corresponding quantities obtained by ten Brinke et al.[4] However, as observed in the computed end density, their calculations systematically predict features that are less pronounced than in our computations.

In addition, we have also examined the center of mass density along the x and the y directions in all three cases. It is expected that these densities should assume a value of unity everywhere since there are no constraints in these directions. This was the obtained result, within the standard deviations associated with the calculation of these quantities, providing another check of the reliability of these calculations.

Having examined the densities of the centers of mass of chains in the film the next quantity that was calculated was the second moment of the distribution of the chain segments about the center of mass. This is the mean-squared radius of gyration $[R_G^2(x_{CM},y_{CM},z_{CM})]$ of the chains. Previously,[2] it was found for a confined polymer melt of a single chain length ($n_b = 100$) and plate separation (51σ) that the z component of R_G, $R_{G,z}$, near the surface, was smaller than its bulk value, while the average of the x and y components, $R_{G,x-y}$, was larger than its isotropic value. Also, one had to proceed roughly $2R_G$ from the surface before the z and the x–y components of the radius of gyration assume their isotropic values. We now examine the effects of plate separation on these results. In Figure 4 we plot $R_{G,z}$ for chains of $n_b = 100$ at the three different plate separations as functions of the absolute, normalized distance of the centers of mass of the chains from the walls, ξ_{CM}.

The $R_{G,z}$ of all chains near the surface are significantly smaller than the corresponding value in an isotropic phase. These results are, in addition, apparently independent of plate separation. As expected, the $R_{G,z}$ values in the two narrower films do not ever reach their isotropic values. The essential conclusion from this figure is that chains in the vicinity of the surface are squeezed in a direction perpendicular to the wall. The interface therefore corresponds to a region where chain structure evolves gradually from nearly two-dimensional shapes (small $R_{G,z}$) to an isotropic, three-dimensional form.

The trend observed for $R_{G,x-y}$ is not illustrated here since its behavior is relatively uninteresting. As noted

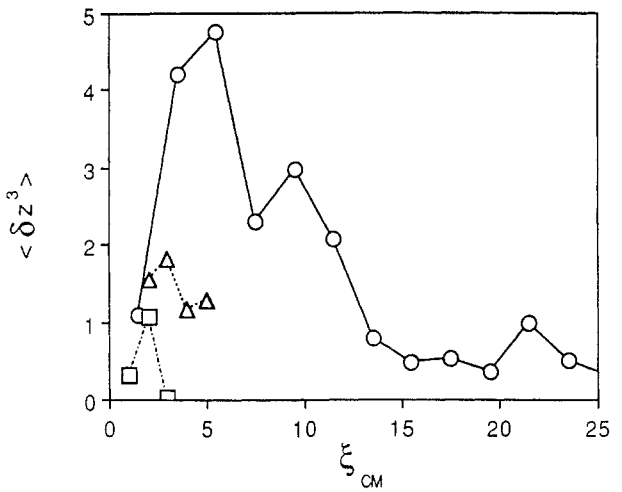

Figure 5. Absolute values of the z component of the third moments of the chains as a function of the absolute, normalized center of mass distance, ξ_{CM}, from the plates. All data are for chains of n_b = 100 with (○) for $D = 51\sigma$, (△) for $D = 11\sigma$, and (□) for $D = 6\sigma$.

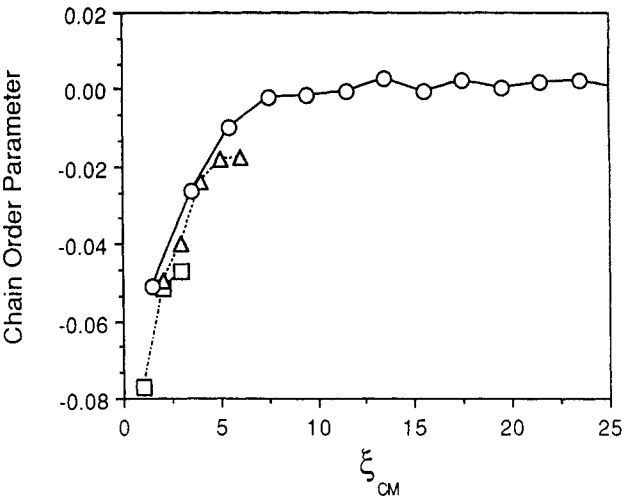

Figure 6. Order parameters of the chains as a function of the absolute, normalized center of mass distance, ξ_{CM}, from the plates. All data are for chains of n_b = 100 with (○) for $D = 51\sigma$, (△) for $D = 11\sigma$, and (□) for $D = 6\sigma$.

earlier,[2] $R_{G,x-y}$ of chains in the immediate vicinity of the surface are larger than the isotropic value. The polymer chains near the wall are thus swollen in a direction parallel to the surface. The total radii of gyrations of the chains were also examined. Consistent with earlier results,[2] it was found that this quantity is independent of the position of the center of mass of the chains. The implication of these results on the conformations of chains in the interface will be discussed later (section 3.3.1).

The R_G results presented above suggest that chains in the vicinity of the surface assumed asymmetric shapes. One appropriate tool to examine this asymmetry is the z component of the third moment of the spatial distributions of segments of a chain about its center of mass. For isotropic chains, all noneven moments should identically be equal to zero. In Figure 5 we plot the absolute value of the z component of the third moment of the chains, $\langle|(\delta z)^3|\rangle$, as a function of ξ_{CM} of the chains for the three different plate separations that have been examined. For the largest plate separation, 51σ, the chains nearest the surface have small third moments. Thus, these chains are essentially symmetric with small tails extending into the isotropic melt. Chains that are roughly one R_G from the surface are the most asymmetric, as evidenced by a large value of $\langle|(\delta z)^3|\rangle$. The chain structures asymptotically become symmetric, as evidenced by a 0 value for the third moment when one proceeds roughly $2R_G$ from the surface. The results from the two other plate separations are then examined in the context of these conclusions.

Similar behavior is observed very close to the surface in the thinner films. Hence, we conclude that the separation of the plates does not play a significant role on the structure of molecules in the immediate vicinity of the surface (i.e., for $\xi_{CM} < 2$). In contrast, the magnitude and the positions of the peaks in the distribution are strongly affected by the thicknesses of the polymer film. The absolute value and position of this peak are seen to decrease from values of ca. 5 at $\xi_{CM} = 5$ ($D = 51\sigma$) to ca. 2 at $\xi_{CM} = 3$ ($D = 11\sigma$) and subsequently to ca. 1 at $\xi_{CM} = 2$ ($D = 6\sigma$). Chain shapes in thin films, on average, are thus more symmetric than chains in thicker films. An explanation of this result is that chains show increased "bridging" between the surfaces as the plate separation is reduced, leading to structures that are more symmetric. In summary, it is emphasized that the third moment is the only quantity that has been examined to this point that is affected significantly when the plate separation is reduced.

The moments of the distributions of chain segments about their centers of mass establishes the spatial distributions of the chain segments. Although the third moment indicates that the chains in the thinner films are more symmetric in shape, it however is not indicative of the average orientations of the chains (relative to the surface) in the interface. A commonly adopted technique to characterize the alignment of molecules is to compute the order parameter of the chain. The direction cosine of the jth segment of the chain relative to the z axis, cos $\theta_{j,z}$, is first computed. This is obtained by determining the dot product of the unit vector joining the centers of the j and $j-1$ beads of the chain with the vector defining the z axis. The order parameter of a chain, s_c, is then determined through the equation

$$s_{c,i} = \frac{3\langle\cos^2\theta_{j,z}\rangle_i - 1}{2} \tag{2}$$

where the ensemble average is taken over all beads of a chain. In Figure 6 this order parameter is plotted against the absolute, normalized distance of center of mass of the chain from the surfaces for the three different plate separations examined. It can be seen that, for all the plate separations, the chains closest to the surface have negative order parameters of the order of −0.1. Thus, these chains are aligned preferentially parallel to the surface. In the thickest film chain orientation becomes asymptotically isotropic, as deduced by a 0 value of s_c, when one proceeds roughly $2R_G$ from the walls. In the two thinner films, however, all the chains are oriented parallel to the surface, a fact that could potentially be verified experimentally through a measurement of the birefringence of a thin sample, for example. The results shown in Figure 6 thus confirm the observations that have been made earlier regarding the overall conformations of chains in the vicinity of the impenetrable surfaces. Also, these results indicate that, as observed earlier, the presence of one surface does not significantly modify chain properties at the other surface even for the thinnest films examined.

The essential theme of the results obtained on single-chain properties for different film thicknesses, therefore, is the apparent lack of significant influence, even at small plate separations, of one surface on the proper-

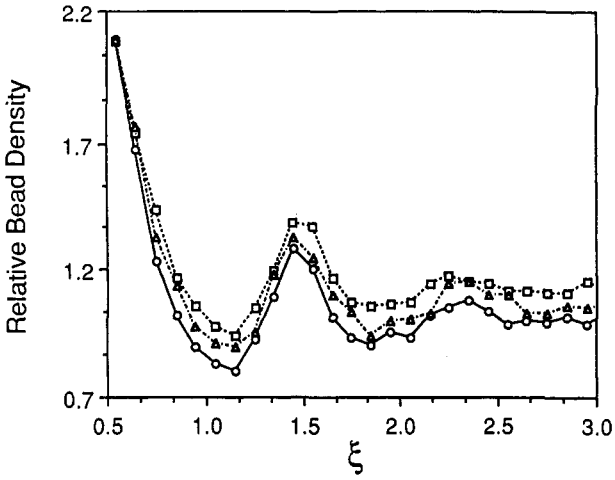

Figure 7. Bead density profiles as a function of their absolute, normalized distance of the layer from the plates. Bead densities have been normalized by the value expected in an isotropic, bulk phase. All data are for chains of $n_b = 100$ with (○) for $D = 51\sigma$, (△) for $D = 11\sigma$, and (□) for $D = 6\sigma$.

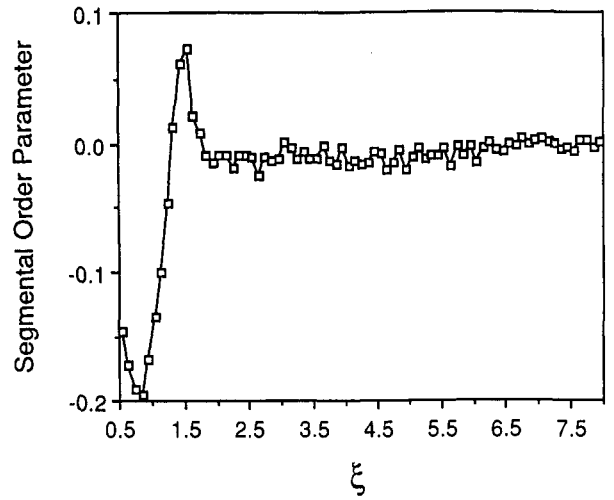

Figure 8. Order parameters of the chain segments as a function of their absolute, normalized distance, ξ, from the plates. This single curve represents data for chains of $n_b = 100$, at three plate separations that have been examined.

ties obtained at the other surface. Although chains in the vicinity of the surfaces remain oriented parallel to the walls, there is evidence that chains participate in the formation of "bridges" between the two surfaces, leading to more symmetric structures as the thickness of the film is decreased. The consequences of this statement will be examined further in the following sections. Additionally, we have shown that one has to proceed roughly $2R_G$ from the plates before chain properties assume their isotropic values. On the basis of single-chain properties, therefore, the interface is ca. $2R_G$ thick.

3.2.2. Properties of Chain Segments as a Function of Their Distance from the Wall. The results that have been presented to this point, i.e., single-chain properties, are qualitatively similar to the corresponding results that have been obtained from lattice calculations.[4] Off-lattice calculations, in addition, allow one to probe single-layer, many-chain properties which determine the thermodynamic properties of the system (like surface pressure and interfacial tensions) in a manner that is more accurate than a lattice calculation. This is due to the fact that a lattice model is inherently limited due to the periodicity that is assumed in its formulation.

To obtain an understanding of the thermodynamic properties of the confined melts, we first computed the density of beads in a layer (normalized by the value expected in an isotropic phase with density that is equal to the average value in the film) as function of the absolute, normalized distance of the layer from the surfaces. These results, which also represent the radial distribution function between the beads and the wall, are illustrated in Figure 7 for the three different plate separations that were examined. There are three striking features apparent in this figure:

(i) The bead density immediately adjacent to the surface is larger than the value expected in an isotropic phase. This is a consequence of the presence of the hard wall that naturally precludes the presence of any molecules with centers less than $\sigma/2$ from it. In addition, the effect of the surface results in oscillations in the bead density, an effect that persists to a distance of ca. 2σ from the surface.

(ii) The asymptotic value of the normalized bead density far from the surface is larger than unity for the two smaller films. This is a manifestation of the fact that the first $\sigma/2$ from each surface is inaccessible to the molecule segments. Hence, there is an enhancement of the normalized density in the volume that is occupied by the centers of the beads.

(iii) The density of beads immediately adjacent to the surface determines the net pressure exerted by the film on the impenetrable, hard surface and hence the force experienced by two plates immersed in a polymer melt. It is seen in Figure 7 that the appropriately normalized quantity, $\rho_b(z)$, is essentially independent of plate separation. This calculation hence suggests that the net pressure exerted by a polymer film on a surface, within the accuracy of the simulation, is independent of plate separation in all cases that have been examined in this work (i.e., for films of thicknesses larger than R_G). Such films thus exert no net force on plates immersed in a melt, a result that is in excellent agreement with lattice calculations[4-6] and experiment.[7] The one point to be emphasized is that these results are contingent on the applicability of the normalization condition used in the calculation of $\rho_b(z)$.

To further characterize the conformations of macromolecules in the interface, we have calculated the order parameter of molecular segments, $s_s(\xi)$, as a function of the distance of the layer from the wall.[2] In Figure 8, this quantity is plotted against the absolute, normalized distance of the layer from the surface, ξ. Only one curve is shown since the order parameters for the three different plate separations are virtually identical on the scale of the graph. Hence, we draw an important conclusion that segment ordering in the vicinity of the surface is unaffected by the thickness of the film. Figure 8 also shows that only those segments that are immediately adjacent to the wall are anisotropic in their average orientations. Close to the wall $s_s(z)$ is negative (ca. −0.2), suggesting that segments in the immediate vicinity of the surface are strongly aligned parallel to the surface. At a distance of ca. 1.5σ from the wall, however, the order parameter is positive: these segments must thus be aligned preferentially perpendicular to the surface. The order parameter, $s_s(\xi)$, assumes its isotropic value of 0 as soon as one proceeds ca. 2σ from the surface. As pointed out previously,[2] these simulation results are in good agreement with the mean-field lattice calculations of Helfand,[10] which predicts that $s_s = -0.22$ in the first layer, 0.02 in the second layer, and 0.0 in the third and the following layers.

In summary, we have, through the use of many-chain, single-layer statistics, demonstrated that the effects of a

Table III
Order Parameter Computed Using Eq 3 Compared to the Order Parameters of Chains As Obtained from the Simulations[a]

center of mass position[b]	$\rho_b(\xi_{CM})$	s_c'	s_c
1.5	0.356	−0.046	−0.053
3.5	0.510	−0.021	−0.028
5.5	0.092	−0.007	−0.011
7.5	0.030	−0.002	−0.003

[a] Representative results for chains of $n_b = 100$ and $D = 51\sigma$. [b] Center of mass positions are in units of σ. Data were obtained by averaging results over layers of thickness 2σ. Hence the data point 1.5σ represents averaging the appropriate data in a layer that spans $0.5–2.5\sigma$.

surface on the orientations and structure of a polymer melt extends to a distance that corresponds to roughly 2σ from the surface. Alternately, this result asserts that even strong perturbations to a melt system are screened out over distances that are comparable to the monomer size, which is also the correlation length in unconstrained systems, an unexpected result.

3.2.3. Discussion. The off-lattice simulations yield results that are devoid of the limitations associated with a lattice model. In particular, many-chain, single-layer properties (like bead density and segment order profiles) obtained from such simulations are more realistic for the systems of interest. As pointed out earlier,[2] the bead density profile is important in determining the net force experienced by two plates immersed in a melt. Lattice calculations, due to their geometric constraints, cannot be expected to provide reliable estimates for this quantity. Our calculations indicate that, to a first approximation, for all cases examined, there will be essentially no forces exerted on two impenetrable plates immersed in a melt. (In our calculations the minimum film thickness examined corresponded to the R_G of the chains.)

Another important conclusion that can be drawn from the simulations regards the conformations of macromolecules in the interface. Figure 6 suggests that chains near the surface are aligned preferentially parallel to the wall, as implied by a negative order parameter, and that this effect persists for all chains whose centers of mass are located within $2R_G$ from the surface. Figure 8, however, implies that only those chain segments within the first ca. 2σ from the surface are anisotropic in their orientations. The combination of the results from both these figures therefore suggests that chains near the surface assume anisotropic orientations *only due to the segments that are immediately adjacent to the surface*. Since the average span of a chain is ca. $2R_G$, this apparently explains the observed results for chain order parameters, which approach 0 only for those chains that have centers of mass farther than $2R_G$ from the surface.

To verify the assertion presented above we have performed a simple calculation. Following Figure 8 it was assumed that only the segments in the first 2σ thick layer from the wall had a nonzero order parameter. The bead density weighted average segmental order parameter in this 2σ thick layer was computed. (This is termed $s_{s,surface}$.) Then, the fraction of segments in this volume that belong to chains having centers of mass in different lattice layers, $\rho_b(\xi_{CM})$, was calculated. This result has been reported earlier[2] and is also presented in Table III. The order parameter of chains in this approximation, s_c', was then computed through the equation

$$s_c' = \rho_b(\xi_{CM}) s_{s,surface} / \rho_{CM}(\xi_{CM}) \quad (3)$$

where $\rho_{CM}(\xi_{CM})$ is the center of mass density at an absolute, normalized distance of ξ_{CM} from the surface (Figure 3). In Table III we compare the order parameter of chains computed in this fashion with the corresponding quantities obtained directly from the simulation. It is seen that the calculated order parameter (following eq 3) are in quantitative agreement with the results obtained from the simulation. We have performed the same calculation on the two other plate separations that have been simulated in this work, and the results in both these cases are also in excellent agreement with the exact results.

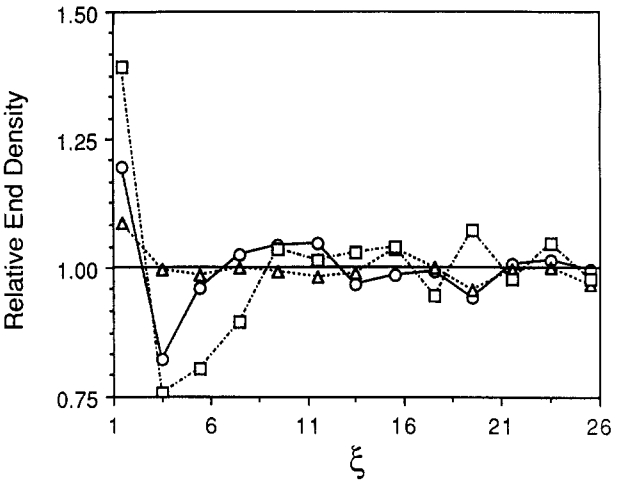

Figure 9. Relative density of chain ends as a function of absolute, normalized distance, ξ, from the plates. End density has been normalized by the value expected in an unperturbed bulk. All data are for a plate separation of $D = 51\sigma$ with (△) for chains of $n_b = 50$, (○) for $n_b = 100$, and (□) for $n_b = 200$.

This calculation therefore has important consequences on the conformation of macromolecular melts near surfaces. We conclude that the only apparent effect of the surface is to perturb the segments within the first 2σ from it. All other segments assume completely isotropic, or random, orientations. Perturbations caused on single-chain properties thus follow purely from the segments in the immediate vicinity of the surface.

3.3. Effects of Polymer Chain Length. In this aspect of the work we have examined the effects of variations in polymer chain length, at a constant value of plate separation ($D = 51\sigma$), on the macroscopic properties observed for these confined systems. Three different chain length polymers were examined: these were of n_b 50, 100, and 200. As usual, we begin by examining the normalized density of ends as function of the absolute, normalized distance from the surfaces (ξ). This is illustrated in Figure 9. As in earlier calculations (ref 2 and section 3.2), the density of ends at the surfaces is larger than the corresponding value in an isotropic bulk. In addition, the density of ends reaches its isotropic value when one proceeds ca. $2R_G$ from the surfaces. These results confirm the trends that have been reported earlier[2] and verify that the appropriate correlation length for this property is the unperturbed radius of gyration of the chains.

The more interesting aspect that emerges from this study is that the enhancement of density of ends immediately adjacent to the surface is larger for longer chain lengths. We have been able to fit this amplification of end density at the surface to the n_b of the chains through the simple expression of the form

$$\ln [\rho_e(z = 0) - 1] = -0.45 - 100/n_b \quad (4)$$

The rationale for selecting the form in eq 4 over others is that it predicts an asymptotic value for the enhancement of end density at the surface with increasing chain length. The form of eq 4 is, in part, motivated by the

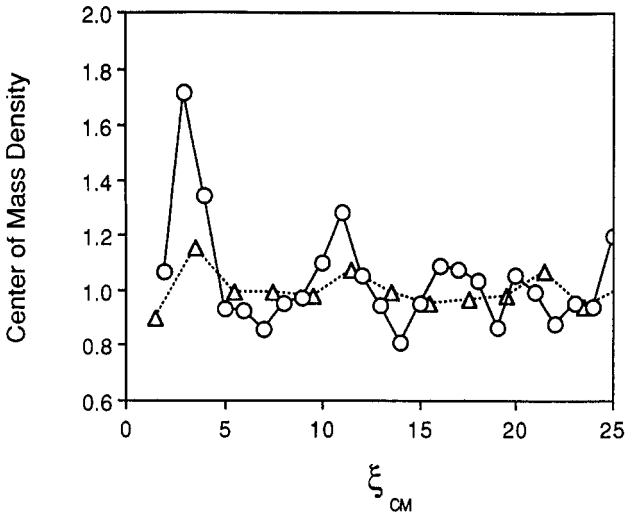

Figure 10. Relative density of chain centers of mass as a function of their absolute, normalized distance, ξ_{CM}, from the plates. Center of mass density has been normalized by the value expected in an unperturbed bulk. All data are for a plate separation of $D = 51\sigma$ with (△) for chains of $n_b = 50$ and (○) for $n_b = 100$.

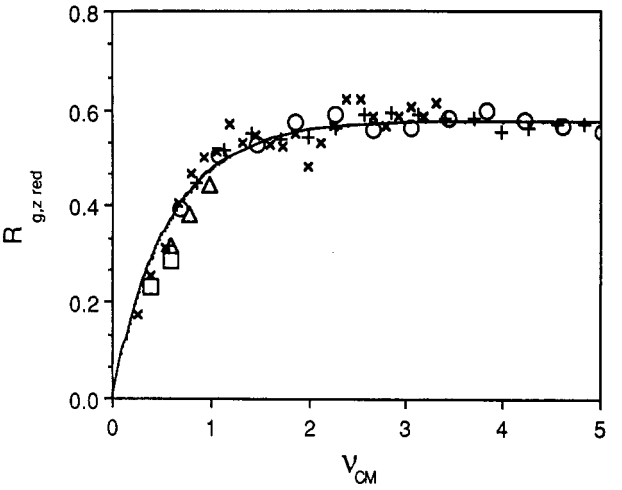

Figure 11. A universal plot of the z component of the radius of gyration of chains in the immediate vicinity of the surface. Data plotted in the form of $R_{G,z,red}$ [$\equiv R_{g,z}/R_G$] vs ν_{CM} [$\equiv \xi_{CM}\sigma/R_G$]. Data from all plate separations and chain lengths have been included, and the line is the prediction of eq 7. Data points are for chains of $n_b = 100$ with (○) for $D = 51\sigma$, (△) for $D = 11\sigma$, and (□) for $D = 6\sigma$, plus those for a plate separation of $D = 51\sigma$ with (+) for $n_b = 50$ and (×) for $n_b = 200$.

lattice calculations of Theodorou,[5] who suggests that the end-density enhancement at the surface does indeed have a finite, asymptotic value for polymers of infinite n_b. Since we have shown in section 3.2 that the density distribution of ends for a single chain length species is independent of plate separation, eq 4 presumably represents a general expression for the enhanced density of end beads at the surface, independent of D. Equation 4 represents a new finding and is not in agreement with the lattice results of ten Brinke et al.,[4] who suggest that the enhancement of end density is independent of chain length and plate separation. In this context it is emphasized that the relationship presented in eq 4 is valid strictly only in the range $50 \leq n_b \leq 200$, although it is likely to be applicable for longer chains. However, it will fail at low n_b, a fact that can be easily verified if one employs a n_b value of 1.

Following ten Brinke et al.,[4] we assume that the preferential partitioning of end beads to the surface is a manifestation of the favorable free-energy change associated with moving an end from the bulk to the surface. We may then write

$$\rho_e(z = 0) = \exp(-U_a/k_BT) \tag{5}$$

where U_a is the appropriate free-energy change in moving an end bead from the bulk to the surface. We can simplify this expression using eq 4 and write the following equation that expresses the adsorption free energy of a chain end as a function of n_b.

$$U_a/k_BT \approx -\ln [1 + 0.64 \exp(-100/n_b)] \tag{6}$$

For chains of infinite length this suggests that the free energy of an end at the surface is roughly $-1/2k_BT$ smaller than in an isotropic phase. The entropic advantage of placing an end bead at the surface rather than in the bulk is thus highlighted by this simple calculation.

3.3.1. Chain Properties as a Function of Center of Mass Position. We begin by examining the normalized density of centers of mass of chains as a function of their absolute, normalized distance from the surfaces. As an illustration, in Figure 10, we plot the center of mass distribution for chains of $n_b = 50$. In comparison to the chains of $n_b = 100$, the peak height of the shorter chains is lower, while chains of $n_b = 200$ (whose results are not shown) demonstrate a higher peak. In addition, this peak occurs at a distance of ca. 3σ from the surface. Again, one has to proceed ca. $2R_G$ from the surfaces before this density assumes its bulk value.

We then proceeded to examine the z and the x–y components of the radius of gyration (R_G) of the three different chain lengths as a function of ξ_{CM}. The qualitative features that were found for chains of length 100 are also observed in this case. The z component of R_G for chains with centers of mass near the surface is small, indicating that these chains are squeezed into essentially pancake-like shapes. Also, it is found that $R_{G,z}$ asymptotically approaches its bulk value as one proceeds to a distance that is comparable to $2R_G$ from the surface.

An interesting aspect of the $R_{G,z}$ data obtained for polymers of different n_b's and plate separations is that they follow an apparently universal behavior when plotted in the form $R_{G,z}/R_G$ vs $\xi_{CM}\sigma/R_G$. Here, R_G is the unperturbed radius of gyration of the chains. In Figure 11 it seen that the data from all the plate separations and chain lengths fall on an essentially universal curve. We have fitted this data with a simple equation

$$3^{1/2}R_{G,z}/R_G = 1 - \exp(-3^{1/2}\xi_{CM}\sigma/R_G) \tag{7}$$

This correlation is illustrated in Figure 11 as a line and can be seen to provide a remarkable fit to the Monte Carlo results. We have thus established the existence of a certain universal behavior of polymer chain properties in the vicinity of a surface. Equation 7 suggests that R_G is the appropriate correlation length for single-chain properties in the vicinity of the wall, consistent with previous arguments.[8,9]

We have also examined the x–y component of R_G in the vicinity of the surface. These results are not reported here because they are relatively uninteresting, except in that they illustrate that coils in the vicinity of the wall are swollen in a direction parallel to the surface.

The z component of the third moments of the chains and the chain order parameters were also studied to delineate the asymmetric shapes and anisotropic orientations of chains in the vicinity of the surface. The general trends observed for chains of length 100 are also seen in this case, and therefore these results are not examined here in detail. We, however, note that the order parameter of chains also seem to follow a universal curve (indepen-

dent of D and the n_b of the chains) when they are examined as a function of $\xi_{CM}\sigma/R_G$. The relationship was of the form

$$s_c = (-1/2R_G)\exp(-3^{1/2}\xi_{CM}\sigma/R_G) \quad (8)$$

Apart from multiplicative prefactors it is seen that the dependence of the order parameter on absolute, normalized distance from the surface has the same functional form as eq 7.

In summary, it was found that single-chain properties near a surface as a function of polymer chain length showed essentially the same trends as have been observed earlier.[2] The order parameter and radius of gyrations of chains were found to obey universal behaviors with the absolute, normalized distance of their centers of mass from the plates scaled by R_G/σ.

3.3.2. Properties of Chain Segments as a Function of Their Distance from the Wall. To study the effects of the surface on the segments of different chain length polymers in the interface we also computed the many-chain, single-layer properties that have been referred to in section 3.2.2. These included the bead density and also the segmental order parameters as a function of the absolute, normalized distance of the layer from the wall.

It was found, within the standard deviations inherent in the calculation of these quantities, that the bead density profile and also the segmental order parameters did not vary with the chain length of the polymer in consideration (see Figures 7 and 8). These results are consistent with the arguments presented in other contexts which suggest that chain properties asymptotically converge to a limit at long chain lengths, a result that indicates the relative unimportance of end effects in truly macromolecular systems.[3] Since the bead density at the surface is independent of chain length, it implies that there is no force exerted on two plates immersed in a melt due to variations in polymer chain length. This statement has important consequences in understanding the effects of polydispersity in the polymer sample on its surface behavior. Our results suggest that, to a first approximation, a distribution of chain lengths in a sample should have almost no effect on properties such as the pressure exerted by the confined melt on the plates.

The results obtained for the segmental order parameters also suggest that the anisotropic orientations of chain segments are restricted to the immediate vicinity of the surface. To verify this conclusion, we have computed the order parameters of chains in a fashion described in section 3.2.3 (i.e., following eq 3). In all cases, reliable predictions for the chain order parameters could be obtained by assuming that segments in the first ca. 2σ from the surface alone exhibited anisotropic orientations. All other segments were allowed to assume random orientations in these calculations. The conclusion of these arguments is that the structure proposed for the interface in confined melts in section 3.2 are verified by these results. In addition, this structure is apparently independent of the chain length of the polymer in consideration, implying that end effects do not play a dominant role in this context.

3.3.3. Discussion. 3.3.3.1. Comparison with Mean-Field Lattice Theory. From our simulations, we have shown that only those chain segments near the wall are oriented preferentially parallel to the surface. To examine this aspect, we graphically illustrate a three-dimensional view of a molecule that has its center of mass close to the wall (Figure 12). All beads that are immediately adjacent to the surface (i.e., within one σ from the surface) are filled. In brief, these molecules are nearly two-dimensional near the wall, which explains the observed behavior of the order parameter of the segments near the surface. However, they do not form compact structures but rather favor the formation of ringlike or stretched structures.

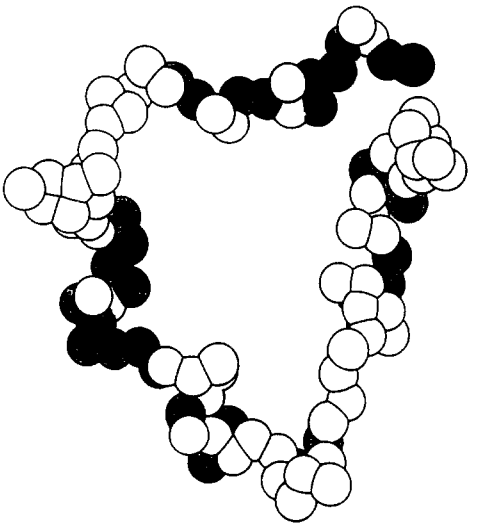

Figure 12. A typical, three-dimensional structure of a polymer chain near the impenetrable surface. The wall lies below the chain, and all beads within 1σ from the wall are filled.

Table IV
Average Length of Surface Train Sequences As Computed from the Simulations[a]

degree of polymerization	sequence length
50	3.85
100	4.09
200	4.25
∞	4.64

[a] Infinite molecular weight results computed from the results of Helfand[10] and Theodorou.[5]

In addition, this structure is an apparently random combination of surface-train sequences and loops.[11] It can also be seen that the loops and surface trains assume a variety of sizes. To characterize the train sequences we have calculated their average sizes and also the distributions of train lengths. This distribution of surface paths (not shown here) indicates that the length of these train sequences follows two-dimensional random walk statistics closely, in good agreement with the simplified analytical model of Ausserre.[6] The computed average length of these surface-trains are shown in Table IV. The average surface-train length for chains of $n_b = 100$ are apparently independent of plate separation and once again demonstrate that plate separation does not play an important role in determining the microscopic structure of the interface. In addition, the last row in Table IV represents the average length of surface-train sequences as predicted by the mean-field lattice theory for noninteracting, infinite n_b chains.[5,11] There are two important facets of these results that should be highlighted. First, the length of the surface sequences is dependent on the chain length of the polymer. However, it can be seen that the results of the surface-train length of the chains asymptotically approach the lattice prediction as one increases the chain length of the confined polymer. In this regard, it should be noted that the segmental order parameters shown in Figure 8 are in good agreement with predictions of the mean-field lattice model of Helfand,[10] which predict $s_1 = -0.22$ in the first lattice layer, $s_2 = 0.02$ in the second lattice layer, and random orientations from

the third layer on. The summary of these results is to emphasize the relevance and applicability of mean-field lattice theories in this context, a completely unexpected result.

3.3.3.2. Molecular Weight Dependence of Surface Tension. We can utilize the information presented in sections 3.3.1 and 3.3.2 to deduce the variation of the surface tension of a melt with the n_b of the chains. We have already shown that the free-energy change associated with moving an end from a bulk phase to the surface can be represented by eq 6. Also, the bead density at the surface is apparently independent of the separation of the plates (Figure 7). Hence, the difference between the surface free energies of a finite chain length system and an infinite chain length system is the free energy associated with moving the appropriate number of ends to the interface. Thus, we can write

$$\gamma a - (\gamma a)_\infty = -U_a \times \text{(moles of ends at the surface/moles of beads)} \quad (9)$$

where a is the average surface area of a chain segment and γ the surface tension of the polymer melt. We may thus write for long chains, following eqs 4–6 that,

$$\gamma a - (\gamma a)_\infty = -k_B T \ln [1 + 0.64 \exp(-100/n_b)](2/n_b)[1 + 0.64 \exp(-100/n_b)] \quad (10)$$

which in the limit of large n_b reduces to

$$\gamma a - (\gamma a)_\infty \propto -k_B T n_b^{-1} \quad (11)$$

This result (eq 11) is consistent with the lattice calculations of Theodorou[5] and suggests that, in the absence of the variation of a with n_b, the surface tension should possess an n_b^{-1} dependence. For long chains it is expected that a, the surface area per chain segment, should be independent of n_b. Thus, it is our prediction that surface tension of a polymer should approach its asymptotic value with increasing molecular weight in a fashion represented in eq 11.

However, this result is not consistent with experimental findings[12] which have suggested that this power law dependence should be $n_b^{-2/3}$. We note that these experimental results were obtained for low molecular weight samples and hence are expected to be influenced by end effects. To examine the behavior of eq 9 at low molecular weights we have studied its predictions over a range of chain lengths. Some representative results are shown in Figure 13. It can be seen that for chains of $200 \leq n_b \leq 1000$ the power law dependence changes continuously but that it can be approximated in this regime by an $n_b^{-2/3}$ dependence. This power law changes continuously as one increases n_b and approaches the n_b^{-1} dependence at high molecular weights. These results are in agreement with the theoretical arguments that have been presented by de Gennes[13] and the experimental results of Anastasiadis et al.[14] for the variation of surface tension of a polymer melt with n_b. There is one essential point that has to be emphasized however: de Gennes' arguments[13] are based on the fact that the enthalpic interaction of the ends with the surface are different from that of the other beads. In our calculations, however, all beads interact with the surface and with other beads identically. Our predictions for the variation of surface tension with n_b is thus a manifestation purely of the entropic freedom of chain ends as compared to other beads. The enthalpic contributions, however, may have to be introduced (added) to explain quantitatively the variation of surface tension with molecular weight.

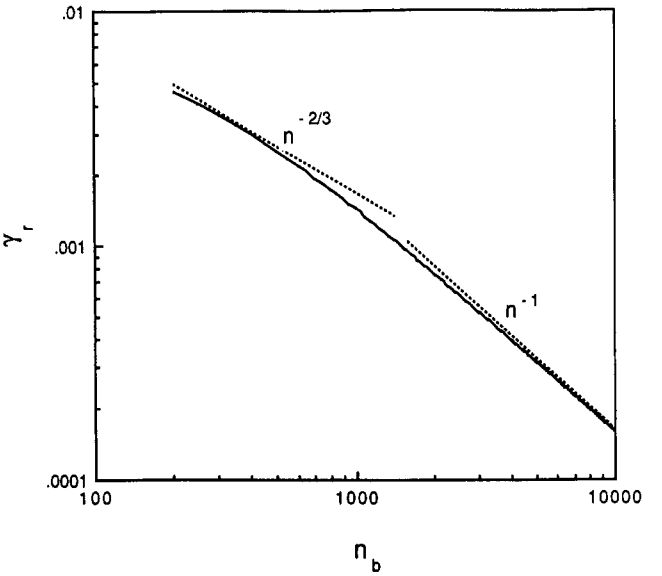

Figure 13. Prediction of eq 10 for the variation of reduced surface tension of a polymer melt, γ_r [$=((\gamma a)_\infty - (\gamma a))/k_B T$], with the n_b of the chains. Lines of slope $n_b^{-2/3}$ and n_b^{-1} are also shown dotted.

Acknowledgment. This work was partly performed when S.K. was a post-doctoral fellow at IBM, Almaden Research Center. We thank IBM Italy for providing financial support to M.V. We also gratefully acknowledge the many useful discussions with Dr. D. Ausserre.

References and Notes

(1) IBM World Trade Visiting Professor. Present address: Dipartimento di Chimica, Universita di Napoli, Via Mezzocannone 4, 80134 Naples, Italy.
(2) Kumar, S. K.; Vacatello, M.; Yoon, D. Y. *J. Chem. Phys.* **1988**, *89*, 5209.
(3) Flory, P. J. *Principles of Polymer Chemistry*; Cornell University Press: Ithaca, NY, 1953.
(4) ten Brinke, G.; Ausserre, D.; Hadziioannou, G. *J. Chem. Phys.* **1988**, *89*, 4374.
(5) Theodorou, D. N. *Macromolecules* **1988**, *21*, 1400.
(6) Ausserre, D. Submitted to *J. Phys (Les Ulis, Fr.)*
(7) Horn, R. G.; Hirz, S. H.; Hadziioannou, G.; Frank, C. W.; Catala, J. M. *J. Chem. Phys.* **1989**, *90*, 6767.
(8) De Gennes, P.-G. *Scaling Concepts in Polymer Physics*; Cornell University Press: Ithaca, NY, 1979.
(9) Madden, W. G. *J. Chem. Phys.* **1987**, *87*, 1405.
(10) Helfand, E. *J. Chem. Phys.* **1975**, *63*, 2192.
(11) Scheutjens, J. M. H. M.; Fleer, G. J. *J. Phys. Chem.* **1979**, *83*, 1619.
(12) LeGrand, D. G.; Gaines, G. L. *J. Colloid Interface Sci.* **1969**, *31*, 162.
(13) De Gennes, P.-G. *C. R. Acad. Sci. Paris* **1988**, *307*, 1841.
(14) Anastasiadis, S. H.; Gancarz, I.; Koberstein, J. T. *Macromolecules* **1988**, *21*, 2980.